ACS OMEGA

http://pubs.acs.org/journal/acsodf

Article

Pressure-Induced Structural Phase Transition in $EuNi_2P_2$

Xuehui Wei and Jianzong Wang*

Cite This: *ACS Omega* 2022, 7, 15200−15205

Read Online

ACCESS | Metrics & More | Article Recommendations | Supporting Information

ABSTRACT: $EuNi_2P_2$ was studied with a diamond anvil cell (DAC) and X-ray diffraction (XRD). The structural evolution of powder crystal $EuNi_2P_2$ under high pressure up to 137 GPa and its single-crystal structure up to 9 GPa were reported. The unique structural phase transition of this 122-type crystal occurred above 70 GPa in powder crystal $EuNi_2P_2$. The diffraction data from single-crystal $EuNi_2P_2$ revealed the coordinate change of the P atom, and the stability of the crystal at 9 GPa was confirmed. The crystal $EuNi_2P_2$ remained stable with a tetragonal phase without obvious symmetry changes during compression to 137 GPa.

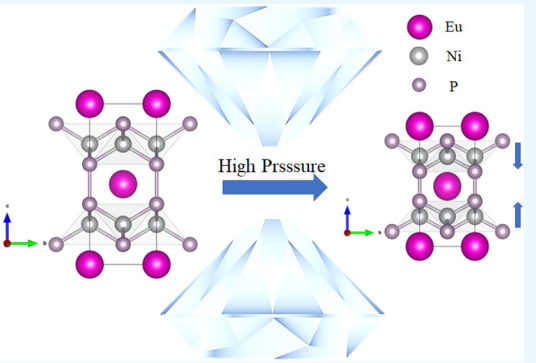

INTRODUCTION

There is a rich variety of compounds similar to the $ThCr_2Si_2$-type crystal ($I4/mmm$). Its unique tetragonal structure can accommodate a variety of atoms with large radius differences, which leads to its special structural and electromagnetic transitions that occur under high pressure.[1−5] According to previous works on high-pressure study of $EuNi_2P_2$, the crystal had no obvious structural change in the pressure range of 32−45 GPa.[5,6] Interestingly, this type of crystal often exhibits a transition to a collapsed tetragonal phase at high pressure, such as $EuCo_2As_2$, $EuFe_2As_2$, or $EuCo_2P_2$. In the phase transition, the abnormal sharp decrease in the *c*-axis parameter has attracted much attention.[3,7,8] The compressibility along the *c*-axis is higher than that along the *a*- and *b*-axes, and high-pressure-induced amorphization may even occur with significant compression along the *c*-axis.[9] In this work, a high-pressure powder crystal X-ray diffraction (XRD) experiment on $EuNi_2P_2$ was carried out to investigate whether there was a similar phase transition to a collapsed tetragonal phase. We investigated the compressibility of $EuNi_2P_2$ under high pressures up to 137 GPa at room temperature. The equation of state (EOS) of $EuNi_2P_2$ was also evaluated by fitting pressure−volume data that had been collected and Rietveld refined. Above 66 GPa, the *c* parameter and crystal volume of $EuNi_2P_2$ suddenly changed and a possible phase transformation occurred.

The valence state of the rare earth element Eu has always been a hot topic in physics and is closely related to the transfer of some 4f-electrons to the conduction band and near the Fermi surface.[10] In recent years, $EuNi_2P_2$ has been regarded as a rare earth compound with a mixed valence state, and the valence state of Eu is closely related to both pressure and temperature.[11] The evolution of the volume of single-crystal $EuNi_2P_2$, which is somewhat connected to its valence state, is an interesting study.[12] High-pressure study of $EuNi_2P_2$ has shown that there is a transition from Eu^{2+} to Eu^{3+} and that a new P−P bond parallel to the *c*-axis can be formed.[5] Additionally, the electrical resistivity of $EuNi_2P_2$ has been reported to abnormally change above 8 GPa.[6] The changes in the mixed valence state and resistivity under high pressure may be accompanied by subtle changes in the structure; however, as reported, there is no obvious change in the structure based on the powder crystal data. Therefore, by taking advantage of high-pressure single-crystal XRD,[13] this work conducted a detailed study on the high-pressure structure of crystal $EuNi_2P_2$.

EXPERIMENTAL DETAILS

The $EuNi_2P_2$ sample was synthesized using the tin-flux method.[5,14] The samples used in the two independent experiments were processed from the same batch of single-crystal samples.

Powder X-ray Diffraction. The in situ high-pressure XRD measurement for powder $EuNi_2P_2$ was performed up to 137 GPa, using synchrotron X-rays with a wavelength of 0.3344 Å at 13-ID-D in APS (Argonne National Laboratory). The powder sample was loaded into a diamond anvil cell (DAC) with a diamond culet size of 100 μm. A Re chip was used as a

Received: March 5, 2022
Accepted: April 13, 2022
Published: April 23, 2022

https://doi.org/10.1021/acsomega.2c01325
ACS Omega 2022, 7, 15200−15205

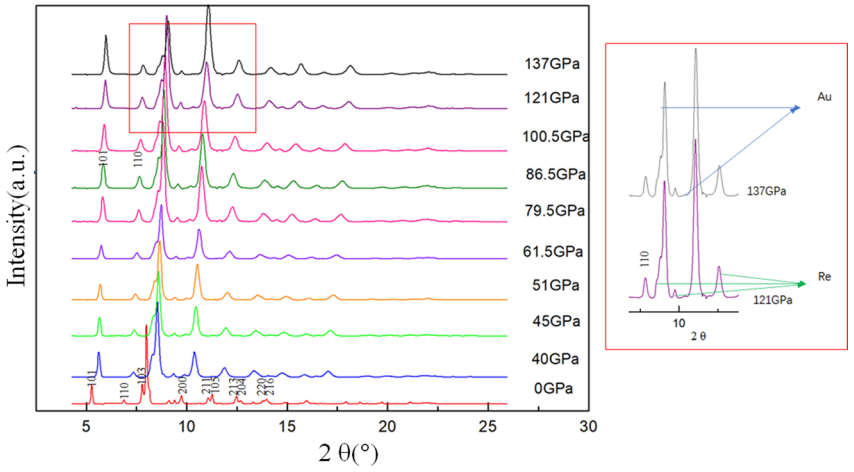

Figure 1. Selected powder synchrotron XRD patterns of $EuNi_2P_2$, with Re and Au pressure markers, up to 137 GPa. X-ray diffraction patterns of $EuNi_2P_2$ at high pressures, which are indexed to the tetragonal $ThCr_2Si_2$-type structure ($I4/mmm$).

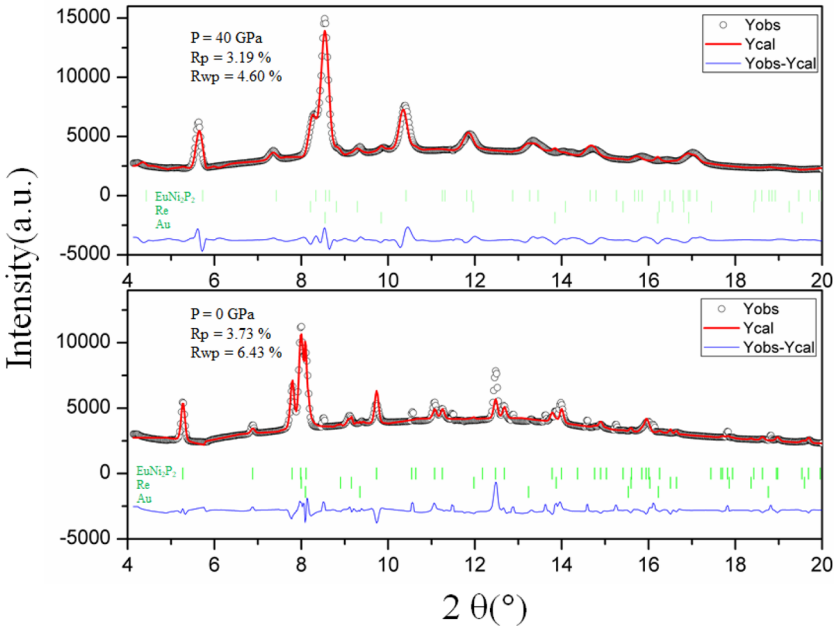

Figure 2. Rietveld refinements of powder $EuNi_2P_2$ (Re, Au) at 0 and 40 GPa showing that no phase transitions are observed up to 137 GPa in the XRD experiments. The crystal is refined according to the ($I4/mmm$, No. 139) symmetry.

gasket, and Au was used as a pressure marker.[15] Without a pressure-transmitting medium, the effects of deviatoric stress present at high pressure will exist.[9,16]

Single-Crystal X-ray Diffraction. For the sample preparation, $EuNi_2P_2$ crystals were processed into 30 μm blocks for later use. The DAC was used as a pressurizing device with a diamond culet of 500 μm. A 300 μm diameter hole was drilled in T301, used as the gasket, to form the sample chamber, and ruby was used as the pressure marker.[17] In this experiment, we loaded neon as a pressure-transmitting medium to offer an approximate hydrostatic environment. The light source used for the experiments was a Bruker D8 VENTURE, a single-crystal X-ray diffractometer with a Ag Kα IμS microfocus source (Ag Kα, λ= 0.56087 Å). The collected data were refined with SHELX through APEX3 and Olex2.[18]

RESULTS AND DISCUSSION

Powder Crystal. Figure 1 shows the diffraction patterns of the powder $EuNi_2P_2$ sample at high pressure, together with those of the Au and Re phases. No obvious new peaks are observed at pressures up to 137 GPa, which proves the stability of this series of crystals.[5−7] No phase transitions are observed up to 137 GPa in the XRD experiments. As shown in Figure 2, the crystal is refined according to the ($I4/mmm$, No. 139) symmetry to obtain the lattice parameters of $EuNi_2P_2$ under pressure. Figure 3 shows the evolution of the lattice parameters during compression and the data from the GSAS and PowderCell program packages.[19] Since there was no pressure-transmitting medium, the initial pressure was 40 GPa. When fitting the volume of the crystal under high pressure using the third-order Birch−Murnaghan EOS,[20] in which the bulk modulus is B_0 and its pressure derivative is B_0', the Birch−Murnaghan formulation is valid only when the latter

https://doi.org/10.1021/acsomega.2c01325
ACS Omega 2022, 7, 15200−15205

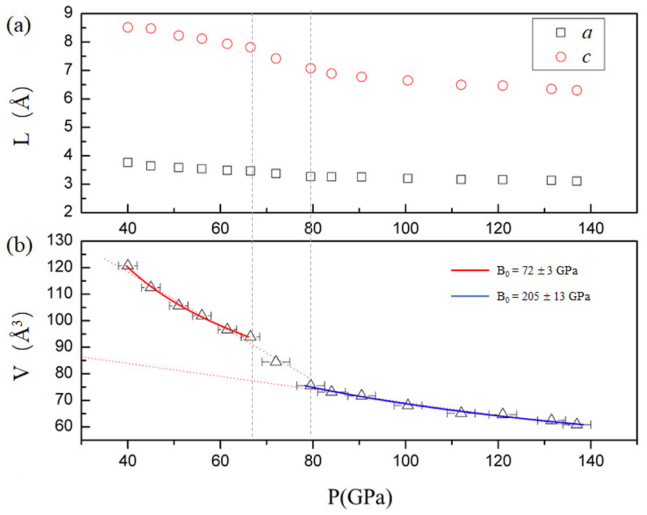

Figure 3. (a) Variations of lattice constants under high pressure. (b) Pressure dependence of the unit cell volume compression (V) for the tetragonal phase of $EuNi_2P_2$ up to 137 GPa. The red and blue solid curves are the Birch–Murnaghan EOS fitted to the two phases. The bulk modulus of $EuNi_2P_2$ is B_0 = 72(3) GPa and 205(13) GPa. The error for pressure determination gradually increases with increasing pressure.

value is sufficiently close to 4,[21] and two red and blue fitting lines can be obtained.

Birch–Murnaghan equation:

$$P = \frac{3}{2}B_0\left[\left(\frac{V}{V_0}\right)^{-7/3} - \left(\frac{V}{V_0}\right)^{-5/3}\right] \times \left\{1 + \frac{3}{4}(B_0' - 4)\left[\left(\frac{V}{V_0}\right)^{-2/3} - 1\right]\right\}$$

In this work, to better compare the bulk modulus of $EuNi_2P_2$, we fitted the obtained volume data to the second-order Birch–Murnaghan EOS (fixing B_0' = 4).[22,23] The correlation coefficient of B_0 and its pressure derivative B_0' in the first fitting is greater than 99%, and that in the second fitting is greater than 98%.[24] However, the bulk modulus B_0 increases to 205(13), which is not only due to the increase in atomic packing in the crystal but also related to the increase in deviatoric stress. The existence of deviatoric stress will reduce the compressibility of the crystal.[9,16] According to Figure 3b, the crystal shows a rapid volume decrease of approximately 19% with the pressure increasing from 66 to 80 GPa; at the same time, the drastic decrease in the lattice parameter c in the crystal is more than 10% according to Figure 3a, which indicates a tetragonal phase-to-collapsed tetragonal phase transition in $EuNi_2P_2$ above 66 GPa. The same type of crystal structure has Eu–Eu exchange interactions in the ab-plane and a helical antiferromagnetic structure with the helix axis along the c-axis direction,[25] where c/a is greater than 2. The material is more compressible along the c-axis under high pressure. Similar to the cases of $EuCo_2P_2$, $EuCo_2As_2$, and $EuFe_2As_2$, in which there is an isostructural collapse in $EuCo_2P_2$ at 3.1 GPa,[3,8] $EuCo_2As_2$ at 4.7 GPa, and $EuFe_2As_2$ at 8.5 GPa,[7] the above structural collapse occurs within 15 GPa. The isostructural collapse of this series is accompanied by negative compressibility of lattice parameter a and reduction of the polar velocity of c, while the high-pressure collapse of $EuNi_2P_2$ only shows rapid compression of c, without negative compressibility of a. According to previous reports, the bond interaction of the P atom and the change in the electronic structure might be the main reasons for the collapse under high pressure.[3] Therefore, more detailed research is needed.

Single Crystal. The high-pressure single-crystal diffraction data are refined to obtain the crystal CIF files within 10 GPa. The evolution of the high-pressure single-crystal parameters is consistent with previous work within 45 GPa.[5,6] As shown in Figure 4, the changes in the a of $EuNi_2P_2$ are relatively stable,

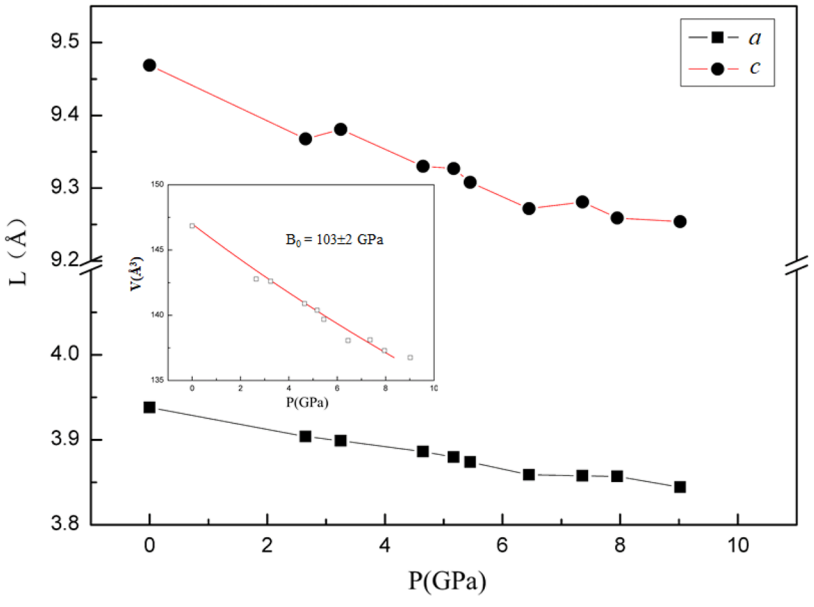

Figure 4. Lattice parameters a and c for the tetragonal phase as a function of pressure; (inset) pressure dependence of the unit cell volume compression (V) for the tetragonal phase of single-crystal $EuNi_2P_2$ up to a pressure of 9.02 GPa. The red solid curves are the Birch–Murnaghan EOS fitted to the phases.

https://doi.org/10.1021/acsomega.2c01325
ACS Omega 2022, 7, 15200–15205

while c fluctuates to some extent, which may lead to instability of the c-axis changes. The single-crystal structure is refined with Olex2 to produce the corresponding CIF files,[18] and the lattice parameters, lattice volumes, and lengths of Ni−P and P−P bonds at different pressures are determined with *pubICIF*.[26] With the Birch−Murnaghan equation,[20] the $P-V$ curve is fitted, and the bulk modulus B_0 is obtained as B_0 = 103(2) GPa. The red solid line in Figure 4 is the Birch−Murnaghan EOS fitted to the phase. Compared to previous reports, the bulk modulus of $EuNi_2P_2$ up to 9.02 GPa is smaller in this work; the previously obtained bulk modulus is B_0 = 154.9(6) GPa in the range of 0−32 GPa[5] and B_0 = 147.9(3) GPa in the range of 0−45 GPa.[6] Interestingly, the single-crystal $EuCo_2As_2$ under nonhydrostatic pressure exhibits an isostructural phase transition from 3.2 to 4.7 GPa with a collapsed tetragonal structure, resulting in a smaller tetragonal structure with bulk modulus B_0 = 48(4) up to 4.7 GPa and B_0 = 111(2) GPa after the collapse.[3] Single-crystal $EuFe_2As_2$, which is layered, also exhibits a collapsed structural transformation, with a smaller bulk modulus of 39(1) GPa before the collapse compared to the value of 134(1) GPa after the collapse.[7] In comparison with the bulk modulus of the same type of crystal, B_0 of single-crystal $EuNi_2P_2$ in the range below 9 GPa of 103(2) GPa has a certain credibility.[23]

The refined high-pressure crystal structure was obtained by Vesta,[27] from which the bond lengths and atomic positions were derived, as shown in Figure 5. The z fractional coordinate

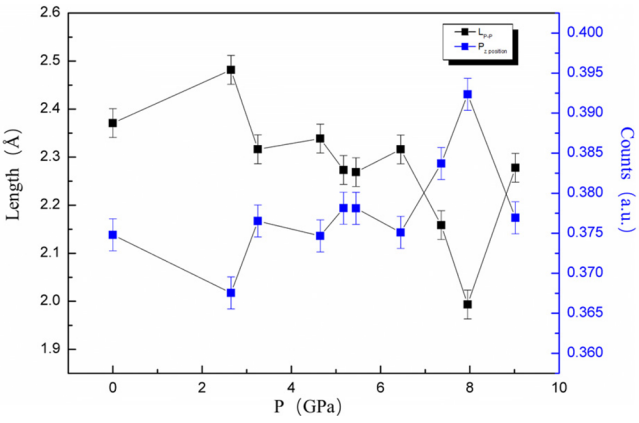

Figure 5. (Blue squares) z fractional coordinate of the P atom; (black squares) evolution trend of the P−P bond length during compression.

of the P atom is the unique changed parameter under high pressure, and the evolution process of the crystal structure under pressure can be better analyzed by studying the evolution of P, which is also an important basis for influencing the fluctuation of the mixed valence state of Eu. The bond length decreases with increasing P atomic coordinate, as shown in Figure 5. There are possible mutations in the crystal during compression due to changes in the valence state that may cause collapsed phase transformation.[28] Possible structural phase transitions can be found by meticulously studying the high-pressure structures.

Medvedev et al. found that the resistivity of $EuNi_2P_2$ obviously changed above 8 GPa.[6] For $ThCr_2Si_2$-type structure $BaTi_2Sb_2O$, a new Sb−Sb bond appears according to the Sb p to Ti 3d bands,[29] and the number of d-electrons is decisive for the order of new bonds.[1] Interestingly, in $EuNi_2As_2$, the existence of Ni vacancies does not affect the crystal structure and related physical properties,[30] but the change in the components will change the lattice volume to some extent and affect the charge transfer efficiency.[31] According to previous work on $EuCo_2P_2$, the crystal structure underwent a collapsed phase transition under 4.5 GPa, and the high-pressure-induced redistribution of the electron density to form a new weak P−P bond. Continuous pressure increased the electron density, and chemical bonds such as Eu−P and P−P were significantly enhanced. For $EuCo_2P_2$ under high pressure, the P−P bond was shortened and the electron redistribution was changed, which eventually led to an obvious change in the crystal microstructure and properties.[4,8] However, in the single-crystal experiment, no fine structural abnormalities of $EuNi_2P_2$ were found during compression to 9 GPa.

As shown in Figure 6, during compression, there appears to be an obvious alteration of the electron density as the pressure

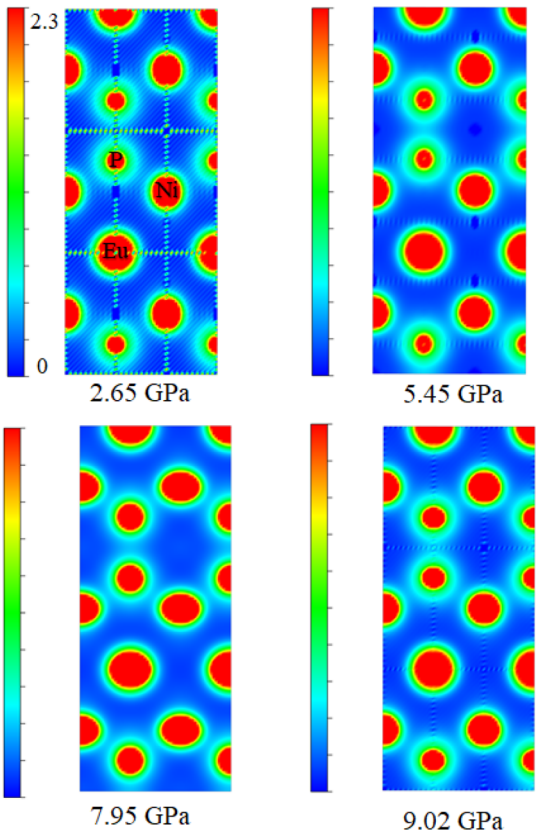

Figure 6. Electron density distribution of atoms (Eu, Ni, P) projected perpendicular to [100].

increases. This electron density alteration coincides with the appearance of charge transfer in previous reports.[3,5−7] Regarding the important role of the d-electrons, in homologous structure $EuFe_2P_2$, both Fe−P and Fe−Fe exhibit covalent and ionic bond characteristics and Fe 3d-electrons also play an important role in the electronic structure.[32] The electronic structure of the Ni (Fe, Co) atom has an important influence on the bond interaction of the anion.

CONCLUSIONS

In this work, the isostructural phase transition of $EuNi_2P_2$ above 66 GPa is found by high-pressure diffraction measurements, and the change in the P−P bond length is found to correspond to the coordinate of the P atom according to the

https://doi.org/10.1021/acsomega.2c01325
ACS Omega 2022, 7, 15200−15205

single-crystal XRD experiment. Due to the large deviatoric stress in the nonhydrostatic environment, the compressibility of $EuNi_2P_2$ is reduced, so we calculated a large bulk modulus B_0 of 205(13) GPa. Combined with single-crystal diffraction data, the symmetry of $EuNi_2P_2$ is found to have good stability but c exhibits a sudden change trend during compression.

■ ASSOCIATED CONTENT

Supporting Information

The Supporting Information is available free of charge at https://pubs.acs.org/doi/10.1021/acsomega.2c01325.

Crystallographic data for $EuNi_2P_2$ at 2.65 GPa (CCDC 2058662) (CIF)

Crystallographic data for $EuNi_2P_2$ at 5.45 GPa (CCDC 2058659) (CIF)

Crystallographic data for $EuNi_2P_2$ at 7.95 GPa (CCDC 2118625) (CIF)

Crystallographic data for $EuNi_2P_2$ at 9.02 GPa (CCDC 2058660) (CIF)

■ AUTHOR INFORMATION

Corresponding Author

Jianzong Wang − *Center for High Pressure Science and Technology Advanced Research, Beijing 10094, China;* orcid.org/0000-0002-4138-4114; Email: 337291543@qq.com

Author

Xuehui Wei − *Center for High Pressure Science and Technology Advanced Research, Beijing 10094, China*

Complete contact information is available at: https://pubs.acs.org/10.1021/acsomega.2c01325

Notes

The authors declare no competing financial interest.

■ ACKNOWLEDGMENTS

We acknowledge the beam time provided at 13-ID-D by APS (Argonne National Laboratory). Experiments were performed on the APS beamline at 13-ID-D with the collaboration of the 13-ID-D staff.

■ REFERENCES

(1) Huhnt, C.; Schlabitz, W.; Wurth, A.; Mewis, A.; Reehuis, M. First- and second-order phase transitions in ternary europium phosphides with ThCr2Si2-type structure. *Phys. B (Amsterdam, Neth.)* **1998**, *252*, 44−54.

(2) Higa, N.; Ding, Q. P.; Kubota, F.; Uehara, H.; Yogi, M.; Furukawa, Y.; Sangeetha, N. S.; Johnston, D. C.; Nakamura, A.; Hedo, M.; et al. NMR studies of the helical antiferromagnetic compound $EuCo_2P_2$. *Phys. B (Amsterdam, Neth.)* **2018**, *536*, 384−387.

(3) Bishop, M.; Uhoya, W.; Tsoi, G.; Vohra, Y. K.; Sefat, A. S.; Sales, B. C. Formation of collapsed tetragonal phase in $EuCo_2As_2$ under high pressure. *J. Phys.: Condens. Matter* **2010**, *22* (42), 425701.

(4) Andersson, P. H.; Nordström, L.; Mohn, P.; Eriksson, O. Theoretical investigation of a pressure-induced phase transition in$EuCo_2P_2$. *Phys. Rev. B* **2002**, *65* (17), 174109.

(5) Li, C.; Yu, Z.; Bi, W.; Zhao, J.; Hu, M. Y.; Zhao, J.; Wu, W.; Luo, J.; Yan, H.; Alp, E. E.; et al. High-pressure synchrotron Mössbauer and X-ray diffraction studies: Exploring the structure-related valence fluctuation in $EuNi_2P_2$. *Phys. B (Amsterdam, Neth.)* **2016**, *501*, 101−105.

(6) Medvedev, S. A.; Naumov, P.; Barkalov, O.; Shekhar, C.; Palasyuk, T.; Ksenofontov, V.; Wortmann, G.; Felser, C. Structure and electrical resistivity of mixed-valent $EuNi_2P_2$ at high pressure. *J. Phys.: Condens. Matter* **2014**, *26* (33), 335701.

(7) Uhoya, W.; Tsoi, G.; Vohra, Y. K.; McGuire, M. A.; Sefat, A. S.; Sales, B. C.; Mandrus, D.; Weir, S. T. Anomalous compressibility effects and superconductivity of $EuFe_2As_2$ under high pressures. *J. Phys.: Condens. Matter* **2010**, *22* (29), 292202.

(8) Yannello, V.; Guillou, F.; Yaroslavtsev, A. A.; Tener, Z. P.; Wilhelm, F.; Yaresko, A. N.; Molodtsov, S. L.; Scherz, A.; Rogalev, A.; Shatruk, M. Revisiting Bond Breaking and Making in $EuCo_2P_2$: Where are the Electrons? *Chem.−Eur. J.* **2019**, *25* (23), 5865−5869.

(9) Wang, P.; He, D.; Xu, C.; Ren, X.; Lei, L.; Wang, S.; Peng, F.; Yan, X.; Liu, D.; Wang, Q.; et al. High-pressure x-ray diffraction study of YBO_3/Eu^{3+}, $GdBO_3$, and $EuBO_3$: Pressure-induced amorphization in $GdBO_3$. *J. Appl. Phys. (Melville, NY, U. S.)* **2014**, *115* (4), 043507.

(10) Franz, W.; Steglich, F.; Zell, W.; Wohlleben, D.; Pobell, F. Intermediate Valence on Dilute Europium Ions. *Phys. Rev. Lett.* **1980**, *45*, 64−67.

(11) Perscheid, B.; Sampathkumaran, E.V.; Kaindl, G. Temperature and pressure dependence of the mean valence of Eu in $EuNi_2P_2$. *J. Magn. Magn. Mater.* **1985**, *47-48*, 410−412.

(12) Hiranaka, Y.; Nakamura, A.; Hedo, M.; Takeuchi, T.; Mori, A.; Hirose, Y.; Mitamura, K.; Sugiyama, K.; Hagiwara, M.; Nakama, T.; et al. Heavy Fermion State Based on the Kondo Effect in $EuNi_2P_2$. *J. Phys. Soc. Jpn.* **2013**, *82* (8), 083708.

(13) Dera, P.; Zhuravlev, K.; Prakapenka, V.; Rivers, M. L.; Finkelstein, G. J.; Grubor-Urosevic, O.; Tschauner, O.; Clark, S. M.; Downs, R. T. High pressure single-crystal micro X-ray diffraction analysis with GSE_ADA/RSV software. *High Pressure Res.* **2013**, *33* (3), 466−484.

(14) Marchand, R.; Jeitschko, W. Ternary lanthanoid-transition metal pnictides with $ThCr_2Si_2$-type structure. *J. Solid State Chem.* **1978**, *24* (3−4), 351−357.

(15) Takemura, K.; Dewaele, A. Isothermal equation of state for gold with a He-pressure medium. *Phys. Rev. B* **2008**, *78* (10), 104119.

(16) Errandonea, D.; Muñoz, A.; Gonzalez-Platas, J. Comment on "High-pressure x-ray diffraction study of YBO_3/Eu^{3+}, $GdBO_3$, and $EuBO_3$: Pressure-induced amorphization in $GdBO_3$" [J. Appl. Phys. 115, 043507 (2014)]. *J. Appl. Phys. (Melville, NY, U. S.)* **2014**, *115* (21), 216101.

(17) Xu, J. A.; Mao, H. K.; Bell, P. M. High-Pressure Ruby and Diamond Fluorescence:Observations at 0.21 to 0.55 Terapascal. *Science* **1986**, *232*, 1404−1406.

(18) Dolomanov, O. V.; Bourhis, L. J.; Gildea, R. J.; Howard, J. A. K.; Puschmann, H. OLEX2: a complete structure solution, refinement and analysis program. *J. Appl. Crystallogr.* **2009**, *42* (2), 339−341.

(19) Toby, B. H. EXPGUI, a graphical user interface forGSAS. *J. Appl. Crystallogr.* **2001**, *34* (2), 210−213.

(20) Vinet, P.; Ferrante, J.; Smith, J. R.; Rose, J. H. A universal equation of state for solids. *Solid State Phys.* **1986**, *19*, L467−L473.

(21) Occelli, F.; Farber, D. L.; Badro, J.; Aracne, C. M.; Teter, D. M.; Hanfland, M.; Canny, B.; Couzinet, B. Experimental evidence for a high-pressure isostructural phase transition in osmium. *Phys. Rev. Lett.* **2004**, *93* (9), 095502.

(22) Li, Y.; Ye, M.; Tang, R.; Chen, J.; Qu, X.; Yang, B.; Wang, X.; Yue, H.; Zhu, P. Pressure-induced isostructural phase transition in Ti_3AlC_2: experimental and theoretical investigation. *Phys. Chem. Chem. Phys.* **2020**, *22* (23), 13136−13142.

(23) Turnbull, R.; Errandonea, D.; Cuenca-Gotor, V. P.; Sans, J. Á.; Gomis, O.; Gonzalez, A.; Rodríguez-Hernandez, P.; Popescu, C.; Bettinelli, M.; Mishra, K. K.; et al. Experimental and theoretical study of dense YBO_3 and the influence of non-hydrostaticity. *J. Alloys Compd.* **2021**, *850*, 156562.

(24) Anzellini, S.; Errandonea, D.; MacLeod, S. G.; Botella, P.; Daisenberger, D.; De'Ath, J. M.; Gonzalez-Platas, J.; Ibáñez, J.; McMahon, M. I.; Munro, K. A. Phase diagram of calcium at high pressure and high temperature. *Phys. Rev. Mater.* **2018**, *2* (8), 083608.

(25) Sangeetha, N. S.; Cuervo-Reyes, E.; Pandey, A.; Johnston, D. C. $EuCo_2P_2$: A model molecular-field helical Heisenberg antiferromagnet. *Phys. Rev. B* **2016**, *94* (1), 014422.

(26) Westrip, S. P. publCIF: software for editing, validating and formatting crystallographic information files. *J. Appl. Crystallogr.* **2010**, *43* (4), 920−925.
(27) Momma, K.; Izumi, F. VESTA 3 for three-dimensional visualization of crystal, volumetric and morphology data. *J. Appl. Crystallogr.* **2011**, *44* (6), 1272−1276.
(28) Yuan, H. Q.; Grosche, F. M.; Deppe, M.; Geibel, C.; Sparn, G.; Steglich, F. Observation of Two Distinct Superconducting Phases in $CeCu_2Si_2$. *Science* **2003**, *302*, 2104−2106.
(29) Yamamoto, T.; Yajima, T.; Li, Z.; Kawakami, T.; Nakano, K.; Tohyama, T.; Yagi, T.; Kobayashi, Y.; Kageyama, H. Pressure-Induced Collapse Transition in $BaTi_2Pn_2O$ (Pn = As, Sb) with an Unusual Pn-Pn Bond Elongation. *Inorg. Chem.* **2021**, *60*, 2228.
(30) Sangeetha, N. S.; Smetana, V.; Mudring, A. V.; Johnston, D. C. Helical antiferromagnetic ordering in $EuNi_{1.95}As_2$ single crystals. *Phys. Rev. B* **2019**, *100* (9), 094438.
(31) Paramanik, U. B.; Bar, A.; Das, D.; Caroca-Canales, N.; Prasad, R.; Geibel, C.; Hossain, Z. Valence fluctuation and magnetic ordering in $EuNi_2(P_{1-x}Ge_x)_2$ single crystals. *J. Phys.: Condens. Matter* **2016**, *28* (16), 166001.
(32) Hua, L.; Shen, J. M.; Zhu, Q. L.; Chen, L. Electronic structure and magnetic coupling properties of $EuFe_2P_2$: First-principles calculations. *Phys. B (Amsterdam, Neth.)* **2011**, *406* (24), 4687−4690.

https://doi.org/10.1021/acsomega.2c01325
ACS Omega 2022, 7, 15200−15205